Simulation of lateral-spread induced piled bridge abutment damage mechanism

E. Stergiopoulou
Graduate Geotechnical Engineer, Athens, Greece (formerly University of Dundee, UK)

J.A. Knappett
Reader in Civil Engineering, University of Dundee, Dundee, UK

L. Wotherspoon
Senior Lecturer, University of Auckland, Auckland, New Zealand

ABSTRACT: The Avondale Road Bridge in Christchurch, New Zealand was extensively damaged due to liquefaction and consequent lateral spreading induced by the Canterbury earthquake sequence (2010-2011). The deck acted as a prop, forcing the abutments to rotate around the deck-abutment connection, causing extensive plastic hinging within the foundation piles and also resulted in extensive settlement in the backfill. In order to further study this observed damage mechanism, key bridge parts were modelled at 1:50 scale including piles made of damageable model reinforced concrete (RC). The soil model was modelled on the layered profile of the south abutment, where the most severe damage was manifested. The model was designed, manufactured, assembled and tested in the University of Dundee (UoD) centrifuge facility. The centrifuge test validated the observed damage mechanism, including the pinning effect of the deck, abutment rotation and backfill settlement, providing a benchmark for future testing of possible retrofit solutions.

1 INTRODUCTION

The Canterbury earthquake sequence that affected Christchurch, New Zealand, in 2010-2011, has re-ignited research in liquefaction and its effects because of its numerous case studies. One of these is the case of Avondale Road Bridge, which crosses the Avon River, connecting the suburbs of Avondale and Burwood (Palermo et al. 2011). Constructed in the early 1960's, it shares typical characteristics with bridge structures built during the same period.

The bridge is 36 m long and 12.8 m wide, carrying two vehicle lanes, one in each direction, and footpaths at either side. Three spans of precast concrete beams constitute the deck, which was originally supported by two L-shaped wall-type abutments at each end, and two intermediate three-column bents on pile caps in the river channel. The abutments, where the most severe damage was reported, were founded on seven 12.2 m long, 406 mm square precast reinforced concrete piles. Four of them were vertical, while three were cast at 14 degrees to the vertical. The intermediate piers were founded on eight vertical 13.7 m long piles (Palermo et al. 2011, Brown, 2011).

The bridge was struck by four main earthquake events during the sequence, which induced lateral spreading of various amounts at the river banks, ultimately damaging the piled abutments beyond repair. It was observed that the deck acted as a prop, forcing the abutments to rotate around the deck-abutment connection. Consequently, the foundation piles were extensively damaged, forming plastic hinges at their connection with the abutments, and this also resulted in extensive settlement in the backfill (Palermo et al. 2011).

In order to further study this damage mechanism, the bridge was modelled at small scale for testing within the University of Dundee (UoD) centrifuge facility. This paper presents the design and manufacturing procedure of the centrifuge model of the existing bridge, introduces the centrifuge testing parameters, and discusses the test results.

2 CENTRIFUGE MODELLING

As mentioned in the introduction, in order to investigate the bridge's damage mechanism, centrifuge modelling was used. This method was selected instead of numerical modelling, because of the model's complexity (i.e. the liquefaction response).

The centrifuge model consisted of the key bridge parts and the surrounding soil model. The former fall into two categories; the first category refers to the reinforced concrete piles of the foundation that were modelled using damageable model reinforced concrete (RC), while the other includes the remaining bridge parts, most of which were modelled for elastic response and manufactured using aluminium alloy. All model components are specified in the following sections.

2.1 *Principles*

The philosophy behind centrifuge modelling is the simplification of a field case into an appropriate prototype, which in turn is scaled down by a factor of *N*, to create the model (Madabhushi, 2015). In this paper, the scale used was *1:50*. The scaling laws are summarized in Table 1.

Table 1. Centrifuge scaling laws (Knappett et al. 2011).

Property	Dimensions	Model : Prototype
Stress (σ)	$ML^{-1}T^{-2}$	1:1
Strain (ε)	1	1:1
Young's modulus	$ML^{-1}T^{-2}$	1:1
Length	L	1:N
Force	MLT^{-2}	$1:N^2$
Bending stiffness (*EI*)	ML^3T^{-2}	$1:N^4$
Bending moment (*M*)	ML^2T^{-2}	$1:N^3$
Time (consolidation)	T	$1:N^2$
Time (dynamic)	T	1:N

2.2 *RC model piles*

The piles' geometry was scaled down by 50, therefore resulting in 240 mm long, 8 mm square model piles, which is the smallest model cross-sectional area ever used using the modelling technique originally introduced by Knappett et al. (2011). The piles were manufactured following a procedure resembling that outlined in Shields (2013) and Al-Defae (2013). The materials used to produce the model concrete mix were Alpha-form plaster (*Crystacal D*, Lafarge Prestia, France), Congleton HST95 silica sand and tap water. The plaster mix, denoted as Mix 3 in Knappett et al. (2011), was mixed at an aggregate/plaster/water ratio of 1:1:0.6 by mass. This mix had a cylinder compressive strength which very closely replicated that of the field piles (40 MPa).

The longitudinal reinforcement was modelled by 4 pieces of 0.58 mm diameter grade 316 stainless steel wire located symmetrically at each of the square section's ends. The transverse reinforcement consisted of 0.26 mm diameter grade 304 stainless steel wire, wrapped around the longitudinal reinforcement, leaving a cover of 1 mm from the model pile's surface. The spacing of the transverse reinforcement was 2 mm over the top 20 mm of length (i.e. at the connection with abutment piece where bending moment and shear are high) and 5 mm for the rest of their length. The key properties of the model piles at prototype scale are compared to the field piles in Table 2. It has to be noted that the transverse reinforcement spacing is different between the field and the prototype piles. This is attributed to two practical reasons; prototype yield strength deriving from the available model wire, and resulting model spacing.

The piles were cast in pairs and were left to cure in air for 28 days prior to their use. The piles intended for use in the centrifuge model were sprayed with Modified Silicone Conformal Coating from RS Components (RS 494-714) in order to become waterproof. Four-point bending tests were conducted on ten further test specimens after spraying with an Instron 5985 loading frame. It was found that the average moment capacity of the tested model piles was only 3% lower than that calculated for the field pile, while they appear to be 19% stiffer in bending than in the field case (Stergiopoulou, 2015). These results are summarised in Table 2. The bending stiffness and moment capacity for the field pile were obtained from a sectional analysis using KSU-RC (Esmaeily, 2015), a reinforced concrete member analysis software.

Table 2. Pile structural properties

Property	Field pile	Prototype
Concrete compressive strength (MPa)	40.0	39.6
Concrete modulus of rupture (MPa)	3.5	3.9
Longitudinal reinforcement:		
Yield strength (MPa)	300	460
Bar diameter (mm)	32	29
Number of bars	4	4
Transverse reinforcement:		
Yield strength (MPa)	300	380
Bar diameter (mm)	13	13
Spacing (mm)	76	250
Structural characteristics:		
Bending stiffness, *EI* (MNm^2)	21.8	26.0
Moment capacity, M_{ult} (kNm)	190	183

2.3 *Remaining key bridge parts*

The remaining parts that were needed to resemble the field case were the deck, which acted as a prop, the abutment, and the hinges that connect these two components (representing the bridge bearings). The deck was modelled according to its axial behaviour in compression. The field deck was a continuous precast post-tensioned unit spanning the entire river and unrestrained from vertical upwards movement (due to deck bowing under compressive load) at the intermediate piers. The full span could not be accommodated in the model container and so Equation 1 needed to be satisfied for similitude to ensure the correct ratio of axial to buckling load (see Table 3):

$$\left(\frac{EI}{L^2}\right)_{field} = \left(\frac{EI}{L^2}\right)_{prototype} \tag{1}$$

where *EI* = bending stiffness; and *L* = deck's length. The deck's model dimensions were finalised as follows: 218 mm long, 85 mm wide and 5 mm thick. The material which was used was aluminium alloy series 6000.

Table 3. Deck structural properties

Property	Field pile	Prototype
Bending stiffness, *EI* (GNm^2)	4.29	0.39
Span (m)	36.25	10.90
EI/L^2 (kN)	3265	3283

The abutment was modelled by geometrically scaling the base geometry and features of the L-wall (the footing component), while the upstanding retaining wall component was modelled to achieve approximate similitude of bending stiffness. It was not known in the field how much bending moment was sustained in the wall and whether this was sufficient to crack the concrete on the side of the retained soil. As a compromise, KSU-RC was used to assess the *EI* of the field reinforced concrete wall under both uncracked and fully cracked conditions, and the final section selected assuming that half of the moment capacity was induced (i.e. beyond the cracked limit, which typically occurs at around $M \approx M_{\text{ult}}/3$). This resulted in the dimensions as illustrated in Figure 1 (which also shows the attached piles) and properties in Table 4. It should be noted that the small batter angle (14 degrees to vertical) on three of the seven piles was not replicated in the model, with all piles being vertical, as its effects were considered negligible. The piles were all glued vertically into slots machined along the base of the abutment using an epoxy resin, as shown in Figure 1. The exterior faces of the abutment were coated in HST95 sand to approximate the rough interface between the concrete and the backfill soil in the field case.

Table 4. Abutment retaining wall properties

Property	Field (uncracked)	Field (cracked)	Prototype
EI (GNm^2)	8.34	1.36	1.85
E (GPa)	N/A	N/A	70
Thickness (m)	0.61	0.61	0.30

The abutment was connected to the deck through a pair of hinges (Savigny Zinc Bichromated Stainless Steel Hinge, 40 mm x 24 mm x 2 mm, RS Stock No. 448-1497) to represent the low moment restraint provided by the bridge bearings at the deck-abutment connection.

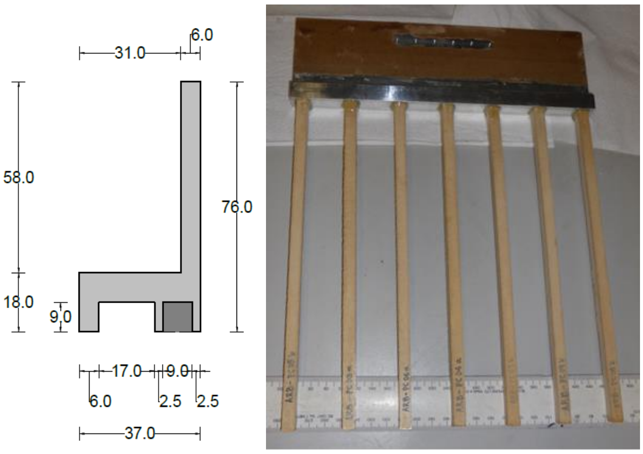

Figure 1. The design of the abutment is presented on the left, featuring its dimensions (in mm, at model scale). The manufactured abutment with the piles permanently glued to the base slots but without the footing component is illustrated on the right.

2.4 *Soil model*

The soil model was designed to approximate the layered profile of the south abutment, as determined from CPTU profiles conducted at the Avondale Road site, where the most severe and most interesting damage was manifested. It consisted of 3 different soil layers. The bottom layer was a 12.65 m thick, medium dense (60% relative density) sand layer. The middle layer was a 1.35 m thick, loose sand layer (25%), while the top layer was a soft silty material 2 m thick with an undrained shear strength of approximately 10-20 kPa (as determined from CPTU tests).

The two sand layers were prepared by air pluviation using Congleton HST95 silica sand within an Equivalent Shear Beam (ESB) container (Bertalot, 2013). A 'slot' pluviator was used for the medium dense sand layer, with its slot opening adjusted to 5 mm. The loose sand layer was then formed on top of the previous layer using a 'spot' pluviator, with the falling height adjusted to 60 mm (Stergiopoulou, 2015). The L-shaped abutment was separated into two parts (the retaining wall and the base/foundation). The sand was pluviated around the assembled retaining wall and piles (Figure 1) which was suspended in place within the container using a temporary mount affixed to the top of the container. After the medium dense layer was complete, the base of the abutment was attached to the retaining wall part using epoxy resin and allowed to fully harden before the loose sand was added above.

It must be noted that the model piles were installed with a different method than in the real bridge, where the concrete piles were driven into the soil. As a result, the model does not replicate the stress history and soil properties around the field piled foundation.

The deck was then attached to the abutment and side of the container before the sand layers were saturated to the top of the loose layer with a viscous fluid of 50 cSt, so that the soil permeability at 50g would resemble that of the soil with groundwater in the field (Bezuijen & Steedman, 2010, Madabhushi, 2015). The viscous fluid was prepared mixing water with hydroxyl-propyl methyl cellulose (HPMC) at a concentration of approximately 2%.

Finally, after saturation the silty layer was added, which was formed from a 40 mm thick crust placed manually on top of the sand layers. It was prepared using A50 Silica Flour and water with a water content of 25%. The slurry was pre-mixed in a tray 400 mm x 280 mm x 65 mm and then was transferred on top of the saturated loose sand layer. This resulted in a non-liquefiable crust with an undrained shear strength between 9-19 kPa as measured using a Controls Group 16-T0175/A hand vane.

3 CENTRIFUGE TESTING

Once complete (Figure 2), the model was loaded onto the UoD beam centrifuge. It is an Actidyn Systemes C67-2 geotechnical centrifuge, with an attached in-flight earthquake simulator (Actidyn Systemes QS67-2). Further specifications for the UoD facility can be found in Bertalot (2013).

3.1 *Instrumentation*

Three different kinds of transducers were utilised. Pore pressure transducers (PPT, *Druck PDCR81*) were used to measure fluid pressures within the soil layers. Micro-Electro-Mechanical Systems (MEMS) accelerometers (*Analog Device ADXL78*) were used for collecting acceleration data. Finally, linear variable differential transformers (LVDT, *RDP Group LDC1000A*) were used externally for collecting displacement data relating to the horizontal movement of the top of the abutment, and its settlement and rotation. More information for them can be found in Stergiopoulou (2015) and Bertalot (2013). The instrumentation was placed in the soil as shown in Figure 2.

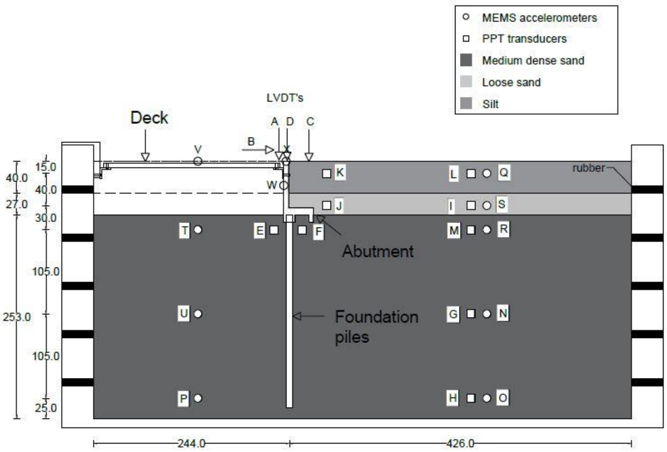

Figure 2. Bridge model and position of instrumentation – side view. The figure presents the bridge model with the three-layered soil, as well as the instrumentation positions.

3.2 *Input data*

The seismic data that were used as input in the centrifuge tests were measured ground acceleration readings from a ‘green-field’ station close to the bridge location (CBGS station at the Christchurch Botanic Gardens, direction N89W). This was a near-surface recording which was applied to the base of the centrifuge container, and so may have been slightly larger than actually experienced around pile tip depth. Four different earthquake motions were used, according to the four major earthquake events that hit Christchurch and damaged the Avondale Road Bridge during the 2010-2011 Canterbury sequence. Their names and the order in which they struck are Darfield, Christchurch, 13 June (a) and 13 June (b). Some details about these earthquakes are presented in Table 5. More information can be found in Stergiopoulou (2015).

It must also be noted that after the Darfield and the Christchurch earthquakes were fired, the centrifuge was stopped and restarted before firing the last two earthquakes. All earthquake motions were fired only after the pore water pressures were observed to have dissipated from post-shake measurements of the PPT data.

Table 5. Main earthquake events of the Canterbury earthquake sequence.

Name	Date	Time (local)	Magnitude (M_w)
Darfield	4/9/2010	04:35:41	7.1
Christchurch	22/2/2011	12:51:42	6.2
13 June (a)	13/6/2011	13:01:00	5.3
13 June (b)	13/6/2011	14:20:49	6.0

3.3 *Output data*

The centrifuge tests provided two ways of investigating the model’s behaviour. One was the inspection of the model after the tests, in order to determine if the overall damage mechanism replicated that observed during post-earthquake reconnaissance and subsequent retrofit of the field bridge. The second was the quantitative output data from the instrumentation, which validate the inspection and provide more insight into the soil’s behaviour, the displacements of the bridge and the overall damage mechanism. The output signals from the instrumentation were recorded on an on-board PC, which was remotely controlled by a PC in the centrifuge control room. The data were collected by a *LabView* routine at a sampling frequency of 4 kHz (Bertalot, 2013).

4 RESULTS AND DISCUSSION

As marked in the previous section, the centrifuge model’s behaviour under the given earthquake motions was documented in two different ways. A selection of these results is presented in this section, teamed in two different categories.

4.1 *Visual observations*

According to the centrifuge testing programme, the centrifuge was stopped after firing the Christchurch earthquake motion, in order to take photos and measurements of the model’s rotation. This motion was the one causing the majority of the damage in the field case. The centrifuge was subsequently reflown for the two 13 June motions before the container was removed from the gondola. The rotation was obvious in both cases, as illustrated in Figures 3 and 4. Rotation measurements were taken with a Fisco Solatronic EN17 Inclinometer at these stages, to complement the LVDT-based data. These post-flight measurements are summarized in Table 6, compared at the same time with the observed values of the field case.

Table 6. Comparison of field and model abutment rotation.

Time interval	Field rotation (°)	Model rotation (°)
After Christchurch	7.7	13.5
After 13 June	9.1	16.2

Figure 3. South abutment photographs taken after the Christchurch earthquake; field (left) and centrifuge model (right).

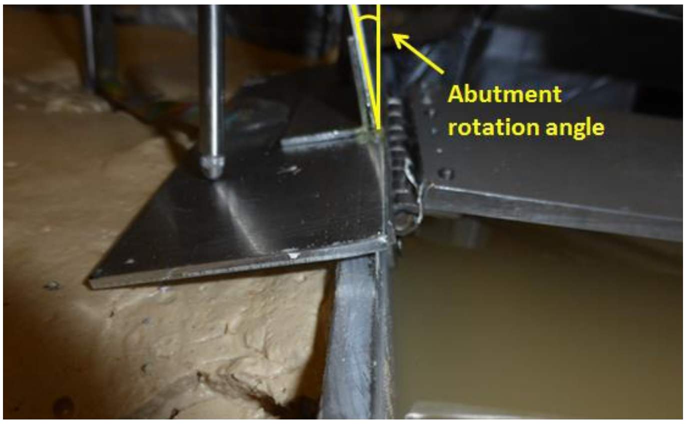

Figure 4. Photo taken at the end of the centrifuge test. The abutment rotation angle is presented.

The centrifuge model appeared to rotate more than the field case (Table 6) but the failure mechanism of 'backwards abutment rotation' with the deck acting as a prop was the same as observed in the post-earthquake field reconnaissance (Palermo et al. 2011). On excavation of the model, excessive bending and permanent deformation of the piles was also observed, as presented in Figure 5. This permanent deformation was measured with a mean value of 22 mm located at the piles' deepest point. Plastic hinges with distinctive cracking on the tension side were formed at the connection of the piles with the abutment, while cracks were also observed at the backfill side of the piles at some depth. In Figure 5 the original position of the piles in relation to the abutment (continuous line) and the original position of the assembly when it was intact (dashed line) are shown to indicate the degree of curvature of the piles and rotation of the abutment, respectively.

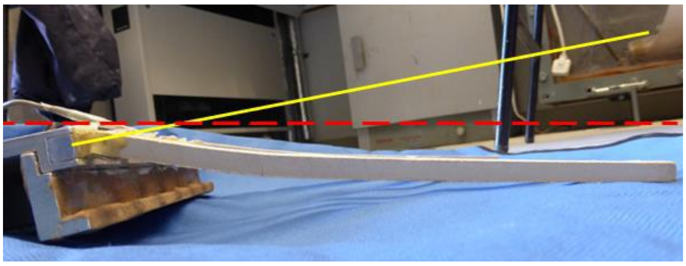

Figure 5. Abutment-piles assembly post-test, where piles' significant bending is apparent. Piles original position referring to the abutment (continuous line) and assembly initial position (dashed line). Both the abutment and the piles rotated.

4.2 *Centrifuge data analysis*

Adding to visual observations, the data gathered by the aforementioned instrumentation was used to verify the observed behaviour. The recorded rotation of the model abutment is shown in Figure 6. It must by noted that the vertical, bold, continuous line in the middle of the figure represents the short break in testing, when the centrifuge was stopped and restarted. Table 6 has already indicated that the centrifuge model rotations were apparently larger than in the field. However, Figure 6 shows that the rotation observed in just the Christchurch (second) event was approximately 8.5 degrees which is very similar to the field measurement after this earthquake. This, coupled with the negligible rotation observed in the field after the Darfield (first) event, suggests that the overprediction of final rotation is a result of overprediction during the first Darfield event. The use of the potentially stronger closest available recording (see Section 3.2) as the input motion may have contributed to this.

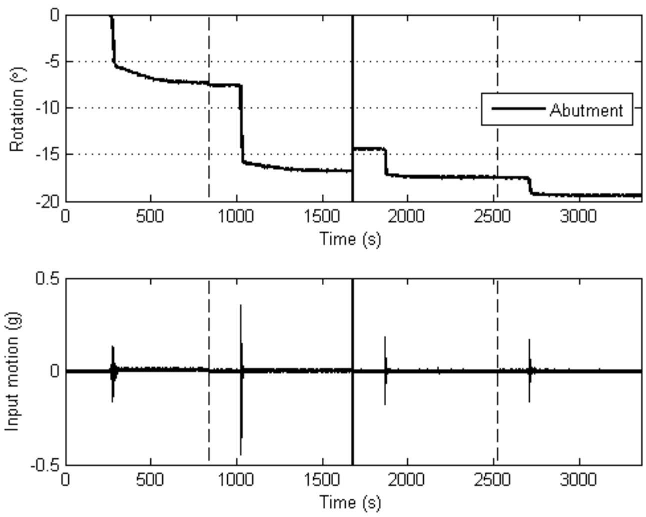

Figure 6. Rotation of the model abutment.

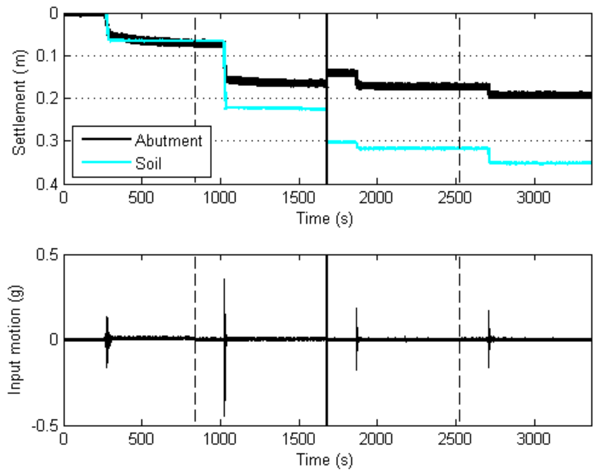

Figure 7. Settlement of the model abutment in comparison with the settlement at the backfill soil.

Settlements of the model abutment and the backfill soil are presented in Figure 7. These indicate negligible differential settlement between the retained soil and abutment in the Darfield earthquake. Following Christchurch, this increases to approximately 70 mm. In the field case, significant cracking of the road pavement was observed above the top of the retaining wall section of the abutment after the Christchurch earthquake associated with a differential settlement of approximately 100 mm, with no pavement damage having been observed after Darfield. These observations are consistent with the centrifuge results.

5 CONCLUSIONS

This paper has described the modelling of a 1960's era piled bridge abutment for a beam-and-slab bridge at a location subject to earthquake-induced liquefaction and lateral spreading (namely, the Avondale Road Bridge case study in Christchurch, New Zealand). The design incorporates damageable elements (precast reinforced concrete piles) for which modelling of the relative soil-pile strength was shown to be important in replicating the damage observed in the field. Through utilising a novel model reinforced concrete developed recently for centrifuge testing at the University of Dundee, along with careful modelling of the other undamaged bridge components and the in-situ soil profile, it was possible to replicate the damage mechanism qualitatively, and obtain quantitative measurements which are representative of the damage induced in the Christchurch Earthquake of 22 February 2011, the most damaging event of the Canterbury Earthquake Sequence. The results of this testing can act as a useful benchmark for the subsequent assessment by centrifuge modelling of potential retrofit solutions for the bridge and comparison to other structural bridge typologies (e.g. ones with integral deck-abutment connections), both of which are currently underway.

6 ACKNOWLEDGEMENTS

The authors would like to thank Mark Truswell for his assistance in model design and fabrication, and in running the centrifuge.

7 REFERENCES

Al-Defae, A.H.H. 2013. Seismic performance of pile-reinforced slopes, PhD Thesis, Dundee: University of Dundee.

Bertalot, D. 2013. Seismic behaviour of shallow foundations on layered liquefiable soils, PhD Thesis, Dundee: University of Dundee.

Bezuijen, A. & Steedman, R.S. 2010. Scaling of hydraulic processes, in Proceedings of the 7th International Conference on Physical Modelling in Geotechnics (ICPMG 2010), 28 June-1 July 2010, Zurich, Switzerland.

Brown, G. 2011. Avondale Road Bridge R104, concept report, SCIRT (Stronger Christchurch Infrastructure Rebuild Team), acquired from Wotherspoon L 2014 pers. comm..

Esmaeily, A. 2015. KSU_RC (online). Available at: <http://www.ce.ksu.edu/faculty/esmaeily/KSU_RC.htm> (Accessed: 12 February 2015).

Knappett, J.A., Reid, C., Kinmond, S. & O`Reilly, K. 2011. Small-Scale Modeling of Reinforced Concrete Structural Elements for Use in a Geotechnical Centrifuge, *Journal of Structural Engineering* 137(11): 1263-1271.

Madhabhushi, S.P.G. 2015. *Centrifuge Modelling for Civil Engineers*, London: CRC Press.

Palermo, A., Wotherspoon, L., Mashal, M., Camnasio, E., Giorgini, S. & Sarti, F. 2011. Qualitative Report for Avondale Rd Bridge, University of Canterbury & University of Auckland, acquired from Knappett JA 2014 pers. comm..

Shields, L. 2013. Small Scale Modelling of Reinforced Concrete for Centrifuge Testing, MSc Thesis, Dundee: University of Dundee.

Stergiopoulou, E. 2015. Damage Mechanisms of Bridge Structures Subject to Lateral Spreading, MSc Thesis, Dundee: University of Dundee.